Zeitschrift Kunststofftechnik
Journal of Plastics Technology

archivierte, rezensierte Internetzeitschrift des Wissenschaftlichen Arbeitskreises Kunststofftechnik (WAK)
archival, reviewed online Journal of the Scientific Alliance of Polymer Technology
www.kunststofftech.com; www.plasticseng.com



eingereicht/handed in: 30.09.2006
angenommen/accepted: 12.01.2007

***Prof. Dr.-Ing. habil. Werner Hufenbach, Dr.-Ing. Bernd Grüber,***
***Dr.-Ing. Albert Langkamp, Dr.-Ing. Martin Lepper, Priv.-Doz. Dr.-Ing. habil. L. Kroll,***
***Institut für Leichtbau und Kunststofftechnik, Technische Universität Dresden***

# *Advanced Calculation Methods for notched Hybrid Composites with Textile-Reinforced Polymers*

*For the description of the notched stress behaviour of hybrid composite structures with glass or carbon fibre textile reinforced polymers, analytical calculation methods are developed at the Institut für Leichtbau und Kunststofftechnik (ILK). The model presented here is based on the enhanced laminate theory combined with the method of complex-valued displacement functions and the method of conformal mappings, from which adapted approaches for the stresses and displacements can be obtained. Extensive experimental research using modern, optical 3D measurement methods is also conducted for the determination of the required material property functions, as well as for verification of the solutions obtained. In addition, the finite element method is utilised for selected parameter combinations as a support. The discussed approach is demonstrated here for the example of hybrid textile-reinforced composite structures being composed of a timber core and textile-reinforced polymer layers on the outside.*

**Autor/author**

Dr.-Ing. Martin Lepper
Technische Universität Dresden
Institut für Leichtbau und Kunststofftechnik
01062 Dresden

E-Mail-Adresse: m.lepper@ilk.mw.tu-dresden.de
Webseite: www.tu-dresden.de/mw/ilk/
Tel.: +49(0)351 463 38 147
Fax: +49(0) 351 463 38 143

# ADVANCED CALCULATION METHODS FOR NOTCHED HYBRID COMPOSITES WITH TEXTILE-REINFORCED POLYMERS

W. Hufenbach, B. Grüber, A. Langkamp, M. Lepper, L. Kroll,
Institut für Leichtbau und Kunststofftechnik, Technische Universität Dresden

For the description of the notched stress behaviour of hybrid composite structures with glass or carbon fibre textile reinforced polymers, analytical calculation methods are developed at the Institut für Leichtbau und Kunststofftechnik (ILK). The model presented here is based on the enhanced laminate theory combined with the method of complex-valued displacement functions and the method of conformal mappings, from which adapted approaches for the stresses and displacements can be obtained. Extensive experimental research using modern, optical 3D measurement methods is also conducted for the determination of the required material property functions, as well as for verification of the solutions obtained. In addition, the finite element method is utilised for selected parameter combinations as a support. The discussed approach is demonstrated here for the example of hybrid textile-reinforced composite structures being composed of a timber core and textile-reinforced polymer layers on the outside.

## 1 INTRODUCTION

Lightweight hybrid composites are often weakened by required cut-outs at various force introduction points or feedthroughs. Here, the ultimate load can be significantly increased by a tailored textile reinforcement with a load-adapted pattern in the disturbing notch area [1], [2], [3]. The stress concentrations of, for example, structures made of textile-reinforced hybrid composites with a usually orthotropic reinforcement is fundamentally different from that of isotropic engineering materials as the former exhibit a strong dependence of the property characteristic, especially on the degree of anisotropy (ratio of stiffnesses parallel and perpendicular to fibre direction), on the composite layers as well as on the lay-up of the textile reinforcement. As a result, uncommon, complicated stress and displacement effects are observed, so that no universal stress concentration factors can be given to the engineer. Instead, the stress concentration factors have to be calculated individually for each lay-up and each load case based on advanced material-adapted calculation methods. Furthermore, the coupling of membrane stress and plate-bending problem occurring with unsymmetrical composites requires an appropriate, more general approach.

The analytical calculation of notched stresses of unidirectionally reinforced composites under mechanical loads has already been conducted by many authors, primarily by means of the method of complex-valued stress functions and the method of conformal mappings. For instance, the notched stress behaviour with tensile/compressive or shear load as well as pure bending load has been treated in [4] dependent on material-specific influence parameters and on the notch contour. A fundamental introduction to this range of problems is provided in [5]. Hygrothermal stress concentration effects have been described in [6] and [7], where additional references concerning the general issue of notched fibre composite plates are also provided. On the other hand, only occasionally authors have studied the analytical notch calculation of multi-layered composites because of the coupling of membrane problems and plate-bending problems arising in the event of unsymmetrical stacking sequences [8], [9]. Among others, Whitney [10] has demonstrated that in this case ignoring the membrane-bending coupling can lead to appreciable errors of up to 300 %. Therefore, a reliable analysis of stress concentrations in textile-reinforced hybrid composites presupposes the consideration of the complete laminate stiffness matrix.

## 2 GENERALISED PLATE EQUATION

For a realistic stress concentration analysis of textile-reinforced hybrid composites, the composite is modelled as an infinite plate with a centric cut-out. Since such structures are considered to be thin-walled, they can be globally described by means of the classical laminate theory. The following structural equation applies for the linear-elastic composite behaviour presupposed here:

$$\begin{pmatrix} N_x \\ N_y \\ N_{xy} \\ \hline M_x \\ M_y \\ M_{xy} \end{pmatrix} = \left(\begin{array}{ccc|ccc} A_{11} & A_{12} & A_{16} & B_{11} & B_{12} & B_{16} \\ & A_{22} & A_{26} & & B_{22} & B_{26} \\ & & A_{66} & \text{symm.} & & B_{66} \\ \hline & & & D_{11} & D_{12} & D_{16} \\ & \text{symm.} & & & D_{22} & D_{26} \\ & & & & & D_{66} \end{array}\right) \begin{pmatrix} \varepsilon_x^0 \\ \varepsilon_y^0 \\ \gamma_{xy}^0 \\ \hline \kappa_x \\ \kappa_y \\ \kappa_{xy} \end{pmatrix} - \begin{pmatrix} N_x^T \\ N_y^T \\ N_{xy}^T \\ \hline M_x^T \\ M_y^T \\ M_{xy}^T \end{pmatrix} - \begin{pmatrix} N_x^Q \\ N_y^Q \\ N_{xy}^Q \\ \hline M_x^Q \\ M_y^Q \\ M_{xy}^Q \end{pmatrix} . \qquad (1)$$

Here, $N_l$, $M_l$ ($l = x, y, xy$) are the stress resultants (forces or moments, respectively), $A_{ij}$, $B_{ij}$, $D_{ij}$ ($i,j = 1, 2, 6$) are the membrane, coupling and bending stiffnesses (respectively), and $N_l^T$, $M_l^T$ as well $N_l^Q$, $M_l^Q$ are the thermally induced or media-induced stress resultants (respectively).

For consideration of the coupling effects of unsymmetrical composites, the Kirchhoff theory is expanded to the so-called Kirchhoff-Love theory by also including the normal stress resultants $N_x$, $N_y$, $N_{xy}$ of the membrane problem into the equilibria of forces and of moments at the differential plate element

$dV = dx \cdot dy \cdot h$ , in addition to the bending loads (resultant moments $M_x$, $M_y$, $M_{xy}$, shear forces $Q_x$, $Q_y$, surface load $p(x, y)$):

$$\frac{\partial N_x}{\partial x} + \frac{\partial N_{xy}}{\partial y} = 0 \quad , \qquad \frac{\partial M_x}{\partial x} + \frac{\partial M_{xy}}{\partial y} - Q_x = 0 \quad ,$$
$$\frac{\partial Q_x}{\partial x} + \frac{\partial Q_y}{\partial y} + p(x,y) = 0 \quad , \tag{2}$$
$$\frac{\partial N_{xy}}{\partial x} + \frac{\partial N_y}{\partial y} = 0 \quad , \qquad \frac{\partial M_{xy}}{\partial x} + \frac{\partial M_y}{\partial y} - Q_y = 0 \quad .$$

The structural law (1) as well as the strain-displacement-relations for small deformations

$$\begin{pmatrix} \varepsilon_x \\ \varepsilon_y \\ \gamma_{xy} \end{pmatrix} = \begin{pmatrix} \frac{\partial u}{\partial x} \\ \frac{\partial v}{\partial y} \\ \frac{\partial u}{\partial y} + \frac{\partial v}{\partial x} \end{pmatrix} = \begin{pmatrix} \frac{\partial u_0}{\partial x} \\ \frac{\partial v_0}{\partial y} \\ \frac{\partial u_0}{\partial y} + \frac{\partial v_0}{\partial x} \end{pmatrix} + z \begin{pmatrix} -\frac{\partial^2 w_0}{\partial x^2} \\ -\frac{\partial^2 w_0}{\partial y^2} \\ -\frac{\partial^2 w_0}{\partial x \partial y} \end{pmatrix} =: \begin{pmatrix} \varepsilon_x^0 \\ \varepsilon_y^0 \\ \gamma_{xy}^0 \end{pmatrix} + z \begin{pmatrix} \kappa_x \\ \kappa_y \\ \kappa_{xy} \end{pmatrix} \tag{3}$$

($u_0$, $v_0$, $w_0$: displacements of the neutral plane)

provide with (2) a generalised plate equation for composites, which comprises a coupling of the membrane and bending problems, and altogether represents a system of coupled partial differential equations (PDE), which was presented in this form for the first time in [8]

$$\underline{\underline{\Delta}} \begin{bmatrix} (A_{ij}) & (B_{ij}) \\ (B_{ij}) & (D_{ij}) \end{bmatrix} \underline{\underline{\Delta}}^T \begin{bmatrix} u_0 \\ v_0 \\ w_0 \end{bmatrix} = \underline{\underline{\Delta}} \left( \begin{bmatrix} (N_i^T) \\ (M_i^T) \end{bmatrix} + \begin{bmatrix} (N_i^Q) \\ (M_i^Q) \end{bmatrix} \right) - (P_i) \ , \tag{4}$$

with the differential operator matrix

$$\underline{\underline{\Delta}}^T = \begin{bmatrix} \frac{\partial}{\partial x} & 0 & \frac{\partial}{\partial y} & 0 & 0 & 0 \\ 0 & \frac{\partial}{\partial y} & \frac{\partial}{\partial x} & 0 & 0 & 0 \\ 0 & 0 & 0 & -\frac{\partial^2}{\partial x^2} & -\frac{\partial^2}{\partial y^2} & -2\frac{\partial^2}{\partial x \partial y} \end{bmatrix} \tag{5}$$

and $(P_i)$ as vector of external loads. For the definition of solutions for this system of PDEs it can be equivalently converted into a single differential equation of the eighth order in $w_0$.

In the special case of a symmetrical composite, the coupling terms $B_{ij}$ in (4) disappear, so that the generalised plate equation is divided into two de-coupled PDEs of fourth order. There, one portion only comprises the bending stiffnesses $D_{ij}$ , and results in the “classic” plate equation for anisotropic materials

$$\left( D_{11}\frac{\partial^4}{\partial x^4} + 4D_{16}\frac{\partial^4}{\partial x^3 \partial y} + 2\left(D_{12} + 2D_{66}\right)\frac{\partial^4}{\partial x^2 \partial y^2} + 4D_{26}\frac{\partial^4}{\partial x \partial y^3} + D_{22}\frac{\partial^4}{\partial y^4} \right) w_0(x,y) = p(x,y) \quad , \tag{6}$$

whereas the other portion only comprises membrane stiffnesses $A_{ij}$, and represents the pure “anisotropic” membrane problem. This may equivalently be presented in the more well-known stress formulation

$$\left( S_{22}\frac{\partial^4}{\partial x^4} - 2S_{26}\frac{\partial^4}{\partial x^3 \partial y} + \left(2S_{12} + S_{66}\right)\frac{\partial^4}{\partial x^2 \partial y^2} - 2S_{16}\frac{\partial^4}{\partial x \partial y^3} + S_{11}\frac{\partial^4}{\partial y^4} \right) F(x,y) = 0 \tag{7}$$

with the (global) membrane compliances $S_{ij}$ according to $[S_{ij}] = h\,[A_{ij}]^{-1}$ and Airy’s stress function $F(x, y)$.

## 3 COMPLEX-VALUED DISPLACEMENT FUNCTIONS AND CONFORMAL MAPPINGS

The method of complex-valued stress or displacement functions in the plane elasticity theory essentially dates back to Kolossow [11], and was later expanded by Sawin [12] to anisotropic plates. Expanding these methods, the solution of the generalised plate equation for multi-layered composites is based on the complex-valued displacement approach for the homogeneous solution and purely mechanical load

$$w_0 = 2\,\mathrm{Re}\left( \sum_{k=1}^{4} \Psi_k(Z_k) \right) , \tag{8}$$

with four analytical functions $\Psi_k(Z_k)$, which are related to four different complex planes $Z_k = x + \mu_k\, y$ ($k$ = 1…4). The complex parameters $\mu_k$ are obtained by inserting (8) into the characteristic equation of the generalised plate equation. Then the eight roots are always pairwise complex conjugates for actual materials, i. e. $\overline{\mu_5} = \mu_1$, $\overline{\mu_6} = \mu_2$, $\overline{\mu_7} = \mu_3$, $\overline{\mu_8} = \mu_4$.

The displacements $u_0$ and $v_0$ ensue from two differential equations which arise during the derivation of the generalised plate equation. The strains $\varepsilon_l$ and curvatures $\kappa_l$ are derived from these displacements with the help of the kinematic relationships (3) and in turn provide the stress resultants $N_l$, $M_l$ ($l = x, y, xy$).

To incorporate the boundary conditions for the stress concentration problem, the notch area is expediently mapped onto the exterior of the unit circle through a conformal mapping $\omega$

$$Z = \omega(\zeta) = R\left(\zeta + \sum_{\kappa=1}^{\infty} \rho_{\kappa} \zeta^{-\kappa}\right) + C \ , \tag{9}$$

whereby the complex figures $R$ and $C$ result in a rotation-stretching or a translation, respectively. The coefficients $\rho_k$ of this series have to be defined suitably. For a description of elementary elliptical notches with the semi-axes $a$ and $b$, e. g., the following equation is sufficient as a conformal mapping:

$$Z = \omega(\zeta) = \frac{a+b}{2}\zeta + \frac{a-b}{2}\frac{1}{\zeta} \ . \tag{10}$$

By expanding the boundary conditions as well as the sought-after solution for the displacement function $w_0$ (8) into Laurent series and by a comparison of coefficients on the notch edge, a linear system of equations is created for the unknown function to be determined.

## 4 CALCULATION RESULTS

The evaluation of the developed analytical solution terms, including the determination of the terms of the series for the conformal mapping, can generally no longer be handled manually [8]. Therefore a computer programme has been created, which performs these calculations and presents the results in a graphic form. As a consequence, the programme enables rapid evaluation of the results and an efficient conduction of parameter studies.

Fig. 1 schematically depicts a symmetrically textile-reinforced hybrid composite sample with a sprucewood base and glass fibre-reinforced plastic (GFRP) layers which is weakened by a circular cut-out.

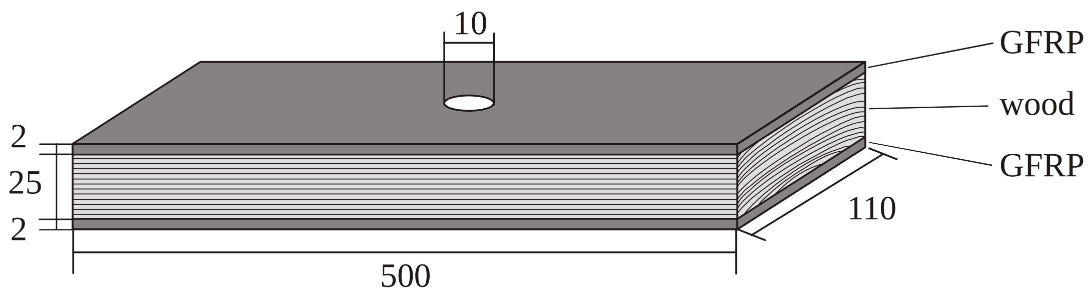


*Figure 1: Schematic representation of a hybrid GFRP/ wood sample with circular hole*

The stress concentration curve of this specimen is presented in Fig. 2 (material properties cf. Table 1).

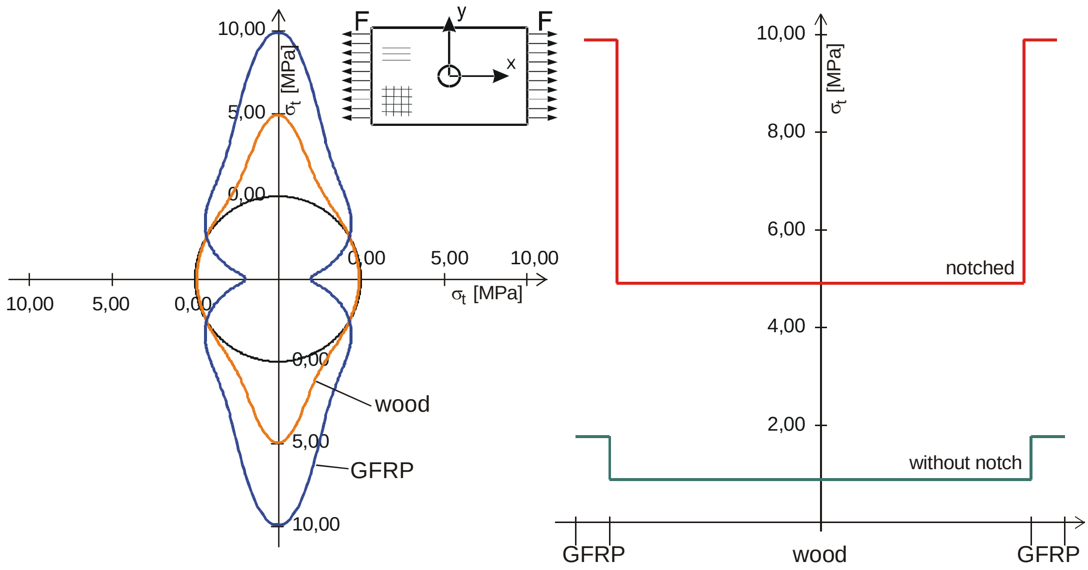


*Figure 2: Analytically-calculated tangential stress for sprucewood with glass fibre-reinforced plastic (GFRP) textile reinforcement*

| Material | $E_1$ [GPa] | $E_2$ [GPa] | $\nu_{12}$ [ – ] | $G_{12}$ [GPa] |
|---|---|---|---|---|
| Sprucewood | 11.9 | 0.79 | 0.323 | 0.6 |
| Glass fibre-reinforced epoxy resins: | | | | |
| Unidirectional (UD) reinforcement | 42.5 | 11.0 | 0.28 | 4.2 |
| Textile reinforcement | 26.9 | 29.9 | 0.115 | 4.2 |
| Multi-axial reinforcement | 21.2 | 21.2 | 0.3 | 8.14 |

*Table 1: Elastic properties of selected timber and GFRP reinforcement materials*

## 5 DETERMINATION OF DIRECTION-DEPENDENT CHARACTERISTIC MATERIAL VALUES

The characteristic material data required for stress concentration analysis, such as Young's modulus, shear modulus, Poisson's ratio and the strength parameters (interaction coefficients, fracture angles and ultimate strengths) of the individual composite layers have been determined in detailed material tests. For some exemplary timber and glass-fibre textile reinforcement materials, Table 1 shows the essential elastic properties; the direction-dependent elasticity modules are compared in Fig. 3.

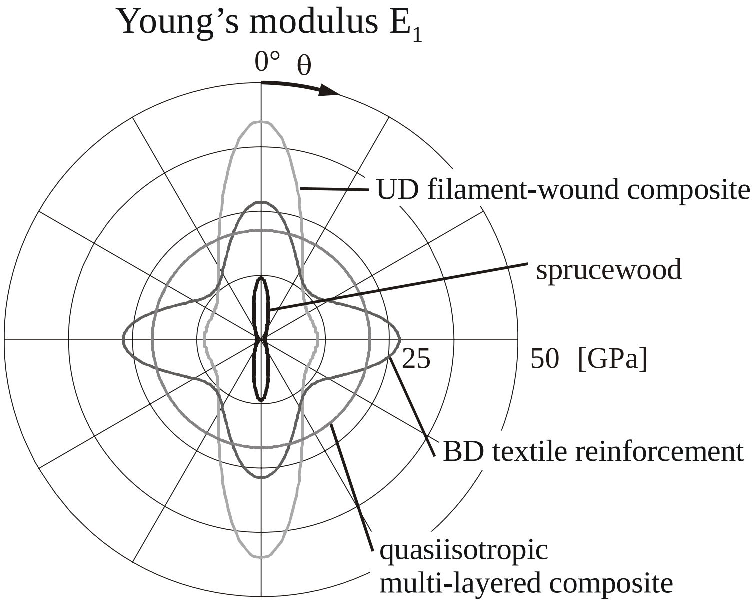


*Figure 3: Comparison of direction-dependent elasticity modules ($\theta$ = 0°: fibre direction)*

The characteristic strength values of glass fibre-reinforced plastic (GFRP) have been determined on flat specimens in the tensile tests or compression tests (respectively) as well as on tube specimens in the tension/compression-torsion test (T/C-T test). In the T/C-T tests, the failure-critical stress combinations along pre-stated load paths were introduced with the help of a specially enhanced load-controlled multi-axial testing machine with adapted strain-twist extensometer, Fig. 4. Normal stress-strain curves as well as shear stress-torsion curves can be prepared with the help of these extensometer measurements.

a)

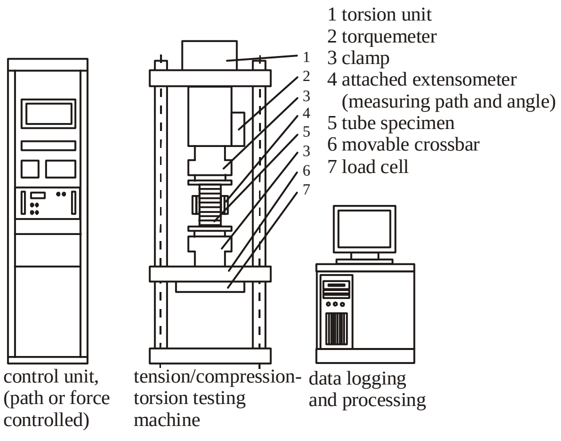


b)

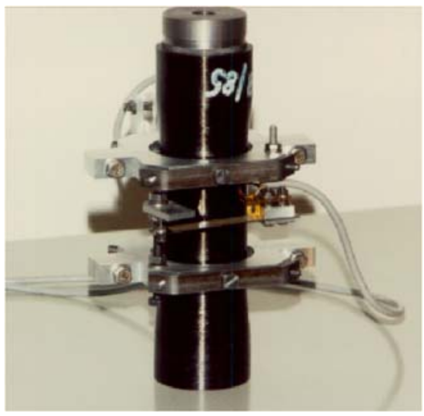

*Figure 4: Tension/compression-torsion failure tests*
*a) T/C-T testing machine,*
*b) Tube specimens with strain-twist extensometer*

In addition, the experiments conducted on filament-wound tube specimens served for the determination of ultimate stresses as well as corresponding fracture angles on the one hand, and on the other hand for the characterisation of elementary types of failure. Furthermore, the additionally obtained information with regard to fracture angle and fracture mode enables a detailed description of the complicated failure phenomena in fibre-reinforced composites. The failure curve in the ($\sigma_2$, $\tau_{21}$) stress plane for unidirectionally reinforced fibre composite materials comprises for example the types of failure: transverse normal failure, transverse-transverse shear failure and transverse-longitudinal shear failure. The considerable amount of information which the T/C-T test supplies allows explaining the initial, essential physical failure phenomena, and on top of that also enables displaying the inadequacies of the general failure criteria, which are quite frequently utilised at present.

The experimental results of the T/C-T tests in tangentially wound fibre/epoxy resin specimens (GFRP: E-Glass/LY556/HT976) for the ($\sigma_2$, $\tau_{21}$) planes are presented in Fig. 5. The load is increased uniformly until failure along pre-determined load paths, for which a constant stress ratio $\sigma_2$ to $\tau_{21}$ is maintained. The measured strengths exhibit a very marginal variance, which indicates a good reproducibility of the experiments. Based on the key strengths $R_\perp^-$, $R_\perp^+$ and $R_{\perp\parallel}$ determined from flat specimens, the failure curve was calculated according to the failure criterion of Hashin/Puck [13]-[15]. This theoretical curve shows a very good congruence with the failure values measured under superimposed loads.

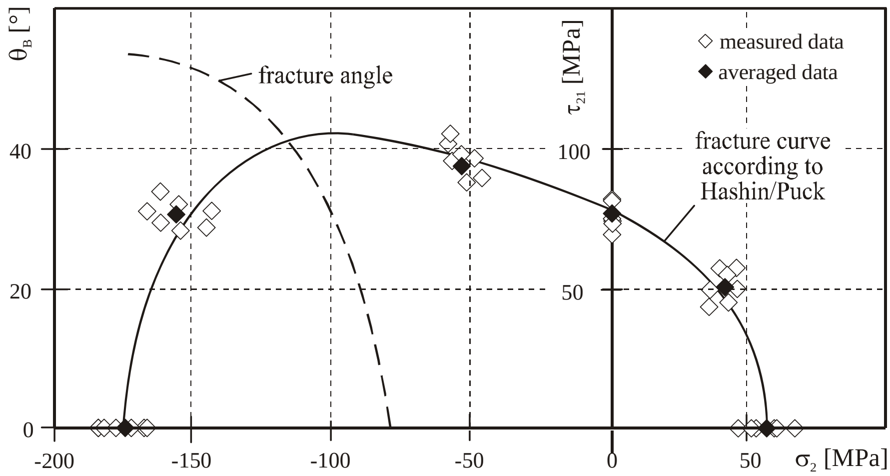


*Figure 5: Strengths, failure curve and fracture angle for tangentially wound GFRP tube specimens*

The slope of the failure curve in the compression/torsion range, which is caused by “internal material friction” according to the hypothesis of Coulomb, is clearly recognisable. Thus it can indisputably be proven that with increasing compressive stress, the shear failure as a consequence of $\tau_{21}$ is increasingly inhibited in the beginning. The gain in compressive stresses thus leads to a change in the relevant failure planes from parallel to the fibre direction to perpendicular to the fibre direction. This results in a relatively strong drop of the failure curve for high compression loads.

## 6 E XPERIMENTAL TESTS FOR VERIFICATION OF THE DEVELOPED SIMULATION MODELS

Extensive load tests are conducted for experimental verification of the developed calculation methods. In particular, the decaying behaviour of the peak stress concentrations is measured and the notched failure is observed with the help of modern 3D field measurement methods such as ESPI (Electronic Speckle Pattern Interferometry) and the grey-value correlation method. The tried and tested strain-gauge technique is applied for reference measurements. Certainly the field measurement methods necessitate a relatively high effort during the implementation and evaluation of the experiment; however, in comparison to the strain-gauge technique they provide not only local values, but details concerning the displacement or strain distribution in the entire field of measurement.

The composite specimens necessary for the bending and tension tests are produced at the ILK on the one hand by means of hand-laminating technique, and on the other hand by the autoclaving method, whereby multi-axial textiles, which have been produced at the Institut für Textil- und Bekleidungstechnik of the Technische Universität Dresden, as well as commercial GFRP plates are utilised as GFRP reinforcement, Fig. 6.

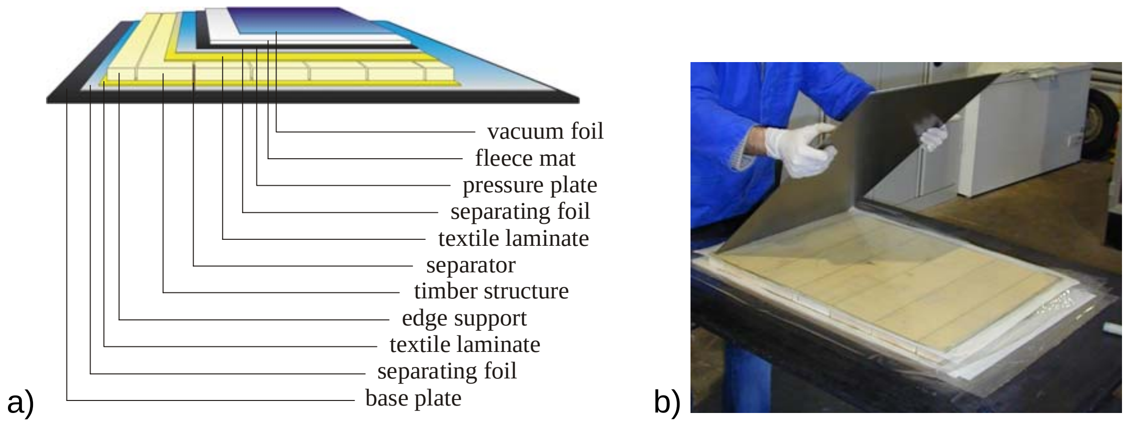


*Figure 6: Manufacture of textile-reinforced timber structures by means of vacuum autoclaving method*
*a) Production layout in the autoclave*
*b) Preparation of the specimen production*

The GFRP/timber structures examined here are equipped with strain gauges at four positions: on the top and bottom surface of the plate, respectively on the x- and y-axis, in 3 mm distance from the edge of the notch, Fig. 7. Usually, 2-axis rosette strain gauges are utilised. $2 \times 5$-point strain gauge chains are also applied on a few selected specimens.

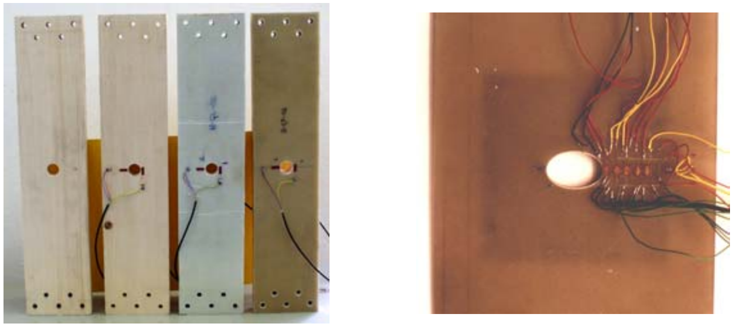

*Figure 7: Strain gauge positioning on the timber-GFRP structures and GFRP specimens*

Fig. 8 shows the strain fields determined by means of the grey-value correlation method for unidirectional GFRP-reinforced timber structures with circular notches loaded in the tension test. The strain fields determined in the experimental tests with membrane loads and plate bending-type loads are then used for verification of the analytical and also numerical simulation models, Fig. 9.

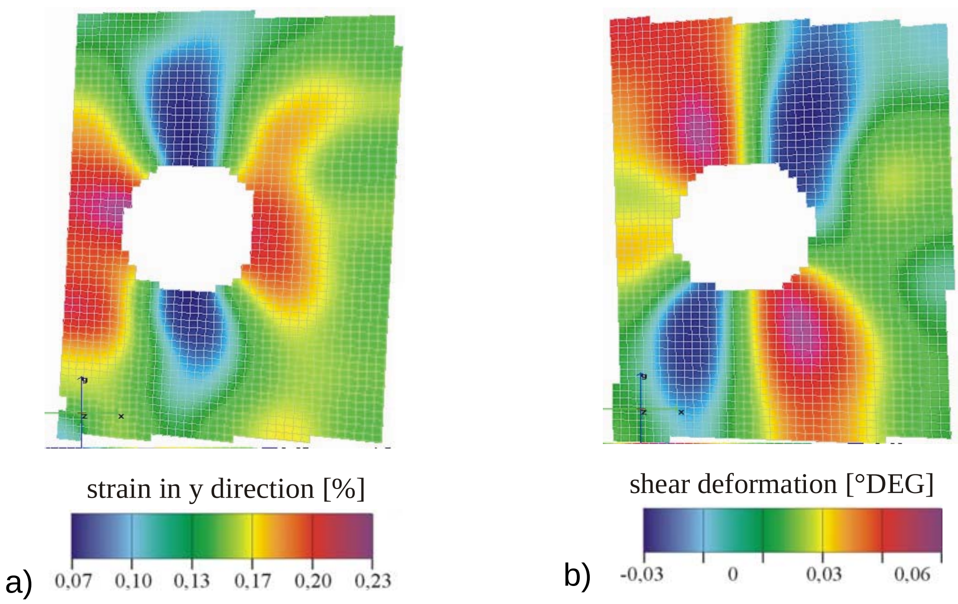


*Figure 8: Strain fields of UD-GFRP timber structures subject to tension*
*a) Strain in load direction $\varepsilon_y$*
*b) Shear strain $\gamma_{xy}$*

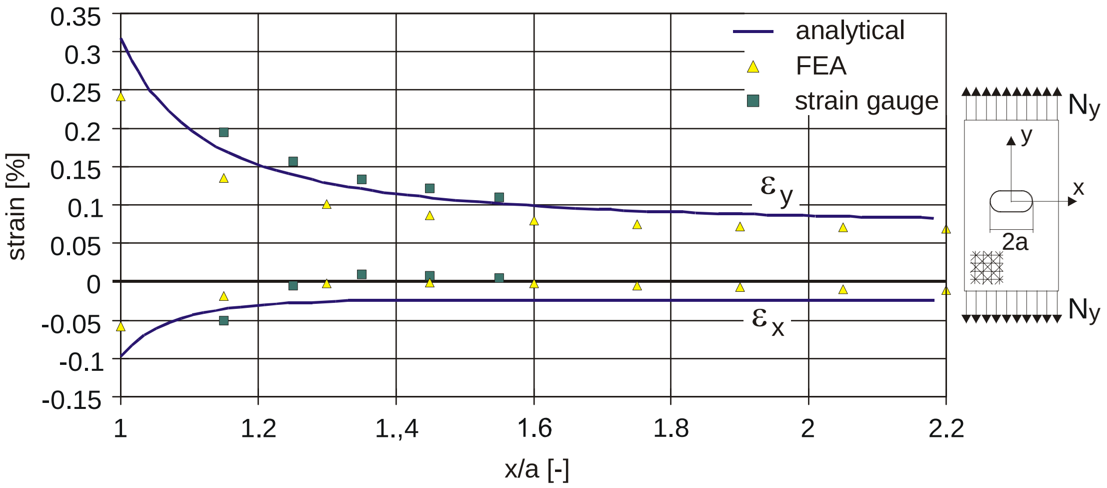


*Figure 9: Comparison of calculated and measured strain for a quasi-isotropic composite*

## 7 CONCLUSION

The developed analytical calculation method for the stress concentration analysis of anisotropic hybrid composites with textile reinforcements subjected to fundamental mechanical loads is essentially based on the method of complex-valued displacement functions in conjunction with the method of conformal mappings. Through expansion of the Kirchhoff theory, the method is modified and expanded to such an extent that the coupling effects of asymmetrical composites, which are unknown for isotropic materials, can also be taken into account.

Altogether, it is illustrated that for treatment of the fundamental boundary value problems presented, the developed analytical solutions are clearly superior to the numerical approach, since, in addition to a reduction of the calculation time, they also allow a certain transparency of the physical context, and thus enable a heightened understanding of complicated notch phenomena. Furthermore, secured, structure-adapted dimensioning formula can be prepared for industrial application on this basis.

Measurements conducted at the ILK reveal a considerable conformity of the analytical, numerical (by means of FEM) and experimentally-determined stress concentration characteristics for multi-layered hybrid composites. Extensive research with regard to verification is currently being conducted at the ILK [16]. The results will subsequently be published in suitable tabular and graphic form, whereby engineers concerned with notch problems in hybrid composites will be provided with an efficient design tool.

**Acknowledgement**

The authors would like to thank the Deutsche Forschungsgemeinschaft for their financial support of the research.

## 8 REFERENCES

[1] Hufenbach, W.; Kroll, L.; Lepper, M.; Langkamp, A. Theoretische und experimentelle Untersuchung textilbewehrter Holzkonstruktionen mit Bohrungen und Ausschnitten Holz (2001) 5, S. D-G.

[2] Hufenbach, W.; Kroll, L.; Lepper, M. Theoretische und experimentelle Kerbspannungsanalyse mehrschichtiger Faser-Kunststoff-Verbunde In: Verbundwerkstoffe und Werkstoffverbunde, Ed. K. Schulte and K. U. Kainer, Wiley-VCH, 1999, p. 103–108

[3] Kroll, L.; Lepper, M.; Grüber, B.; Kostka, P.; Zhou, B. Analytical model for stress and failure analysis of notched hybrid composites 21st International Congress on Theoretical and Applied Mechanics (ICTAM-21), Warschau, 15. –21. August 2004, S. 298

[4] Hufenbach, W.; Kroll, L. Kerbspannungsanalyse anisotrop faserverstärkter Scheiben Archive of Applied Mechanics 62 (1992) 4, p. 277–290

[5] Lekhnitskii, S. G. Anisotropic plates Translation of the second Russian edition. Gordon and Breach, New York et al., 1968

[6] Kroll, L. Zur Auslegung mehrschichtiger anisotroper Faserverbundstrukturen Dissertation, Technische Universität Clausthal, 1992

[7] Hufenbach, W.; Kroll, L. Stress analysis of notched anisotropic finite plates under mechanical and hygrothermal loads. Archive of Applied Mechanics 69 (1999), p. 145–159

[8] Lepper, M. Kerbspannungsanalyse anisotroper Mehrschichtverbunde mit symmetrischem und unsymmetrischem Strukturaufbau Dissertation, Technische Universität Clausthal, 1999

[9] Becker, W. Complex method for the elliptical hole in an unsymmetric laminate Archive of Applied Mechanics 63 (1993), p. 159–169

[10] Whitney, J. M. Structural analysis of laminated anisotropic plates Technomic, Lancaster, 1987

[11] Kolossow, G. V. Über einige Eigenschaften des ebenen Problems der Elastizitätstheorie Z. Math. u. Phys. 62 (1914), p. 384–409

[12] Sawin, G. N. Spannungserhöhung am Rande von Löchern Translation and scientific editing.: H. Neuber. VEB Verlag Technik, Berlin, 1956

[13] Puck, A. Festigkeitsanalyse von Faser-Matrix-Laminaten – Modelle für die Praxis Munich, Carl Hanser Verlag, 1995

[14] Kroll, L.; Hufenbach, W. Physically based failure criterion for dimensioning of thick-walled laminates Applied Composite Materials 4 (1997), p. 321–332

[15] Hufenbach, W.; Kroll, L.; Langkamp, A.; Gude, M. Realistische Festigkeitskriterien für Faserverbundwerkstoffe mit spröder Matrix In: Verbundwerkstoffe und Werkstoffverbunde, Ed. K. Schulte and K. U. Kainer, Wiley-VCH, 1999, p. 319–324

[16] Kroll, L.; Kostka, P.; Lepper, M.; Hufenbach, W. New notched strength criteria for multilayered structures Proceedings of the 11th International Scientific Conference on Contemporary Achievements in Mechanics, Manufacturing, and Materials Science CAM3S, Zakopane, 6.–9. Dezember 2005 (auf CD-ROM)



## Keywords:

Stress concentration analysis, notch, composites, textile-reinforcement


## Kontakt:


Autoren: Dr.-Ing. Martin Lepper



Herausgeber: Prof. em. Dr.-Ing. Dr. h.c. Gottfried W. Ehrenstein, Prof. Dr. Tim A. Osswald

Erscheinungsdatum: März/April 2007

**Herausgeber/Editor:**
Europa/Europe
Prof. Dr.-Ing. Dr. h.c. G. W. Ehrenstein, verantwortlich
Lehrstuhl für Kunststofftechnik
Universität Erlangen-Nürnberg
Am Weichselgarten 9
91058 Erlangen
Deutschland
Phone: +49/(0)9131/85 - 29703
Fax.: +49/(0)9131/85 - 29709
E-Mail-Adresse: ehrenstein@lkt.uni-erlangen.de

Amerika/The Americas
Prof. Dr. Tim A. Osswald, responsible
Polymer Engineering Center, Director
University of Wisconsin-Madison
1513 University Avenue
Madison, WI 53706
USA
Phone: +1/608 263 9538
Fax.: +1/608 265 2316
E-Mail-Adresse: osswald@engr.wisc.edu

**Verlag/Publisher:**
Carl-Hanser-Verlag
Jürgen Harth
Ltg. Online-Services & E-Commerce,
Fachbuchanzeigen und Elektronische Lizenzen
Kolbergerstrasse 22
81679 Muenchen
Tel.: 089/99 830 - 300
Fax: 089/99 830 - 156
E-mail: harth@hanser.de